

19. Manney, G., Farrara, J. & Mechoso, C. The behavior of wave 2 in the southern hemisphere stratosphere during late winter and early spring. *J. Atmos. Sci.* **48**, 976–998 (1991).
20. Bretherton, F. Critical layer instability in baroclinic flows. *Q. J. R. Meteorol. Soc.* **92**, 325–334 (1966).
21. Robinson, W. The application of the quasi-geostrophic Eliassen–Palm Flux to the analysis of stratospheric data. *J. Atmos. Sci.* **43**, 1017–1023 (1986).
22. Randel, W. The evaluation of winds from geopotential height data in the stratosphere. *J. Atmos. Sci.* **44**, 3097–3120 (1987).
23. Thorpe, A. & Bishop, C. Potential vorticity and the electrostatics analogy: Ertel–Rossby formulation. *Q. J. R. Meteorol. Soc.* **121**, 1477–1495 (1995).

Acknowledgements. We thank W. Robinson, K. Emanuel and D. Cunnold for helpful discussions, M. McIntyre for comments and suggestions, T. Kindler and R. Wang for help with data acquisition, D. Haas-Laursen for help with the figures, and K. Evans for comments on an earlier draft. This work was sponsored by NASA/UARS.

Correspondence should be addressed to D.E.H. (e-mail: hartley@eas.gatech.edu).

Simulated future sea-level rise due to glacier melt based on regionally and seasonally resolved temperature changes

J. M. Gregory* & J. Oerlemans†

* Hadley Centre, Meteorological Office, London Road, Bracknell, Berkshire RG12 2SY, UK

† Institute for Marine and Atmospheric Research, Princetonplein 5, 3584 CC Utrecht, The Netherlands

Climate change is expected over the next century as a result of anthropogenic emissions of greenhouse gases and aerosols into the atmosphere, and global average sea level will consequently rise. Estimates¹ indicate that by 2100 sea level will be about 500 mm higher than today as a result of global warming, with thermal expansion of sea water accounting for over half of this rise. The melting of glaciers and ice sheets will contribute much of the remainder. We present an improved calculation of glacier melt, which uses the temperature patterns generated by a coupled atmosphere–ocean general circulation model^{2,3} as inputs to a seasonally and regionally differentiated glacier model^{4,5}. Under specified greenhouse-gas and sulphate-aerosol forcings, our model predicts that glacier melt equivalent to 132 mm of sea-level rise will occur over the period 1990–2100, with a further 76 mm from melting of the Greenland ice sheet. These figures fall within the range of previous estimates made using simpler models¹; the advantage of our approach is that we take into account the effects of regional and seasonal temperature

variations. Our inclusion of these effects increases the calculated glacier melt by 20%.

The atmosphere–ocean general circulation model (AOGCM) used in this work is the HADCM2 model of the Hadley Centre². Both the atmosphere and the ocean components are grid-point models with a spatial resolution of 3.75° of longitude by 2.5° of latitude. The Greenland and Antarctic ice sheets are represented by a permanent layer of snow. Like other AOGCMs, HADCM2 does not include any smaller ice caps or glaciers, which are assumed to have negligible climatic influence on the large scale.

Two simulations ('SUL' and 'GHG') were made of time-dependent climate change from 1860 to 2100 (refs 2, 3; Fig. 1) forced with estimates of the historical and future increase of greenhouse gases. SUL also included the effect of sulphate aerosols, which cool the climate system by reflecting solar radiation. The global average temperature rise from 1990 to 2100 was 2.7 K in SUL, 3.3 K in GHG. Previous results⁶ for the temperature rise if aerosol is included span the range 1.0–3.5 K, reflecting both the differences among the scenarios used for emissions for greenhouse gases and aerosols, and the uncertainty in the response of the climate system, particularly in the effect of aerosol.

The glacier model calculates the rate of change dV/dt of world glacier volume (expressed as the equivalent volume of liquid water) due to glacier melt during year i (time t_i) as

$$\frac{dV}{dt} = \sum_{j=1}^n A_j \left(\Delta T_s(\mathbf{x}_j, t_i) \frac{dB}{dT_s}(\mathbf{x}_j) + \Delta T_N(\mathbf{x}_j, t_i) \frac{dB}{dT_N}(\mathbf{x}_j) \right)$$

which is a sum over $n = 100$ glaciated regions (Fig. 2)^{4,5}. The j th region is located at \mathbf{x}_j (longitude, latitude), and has glacier area A_j and time-independent mass balance sensitivities dB/dT_s and dB/dT_N (always negative) to changes ΔT_s and ΔT_N , with respect to the unperturbed climate, in the average temperature of the summer and non-summer months. ('Summer' is June–July–August in the Northern Hemisphere, December–January–February in the Southern Hemisphere.) The 'mass balance' B (dimensions of metres per year) of a glacier is the rate at which it is changing its total mass (water volume equivalent) divided by its surface area. A 'mass balance sensitivity' is simply the derivative of B with respect to a climate parameter that affects it.

The sensitivities depend on present local climatological precipitation, through a relationship derived from the results of an energy–balance model calibrated for a number of individual glaciers representing a variety of climate regimes⁷, taking into account their hypsometry (area–altitude distribution). Glaciers in regions of high precipitation have a higher mass-turnover and extend to

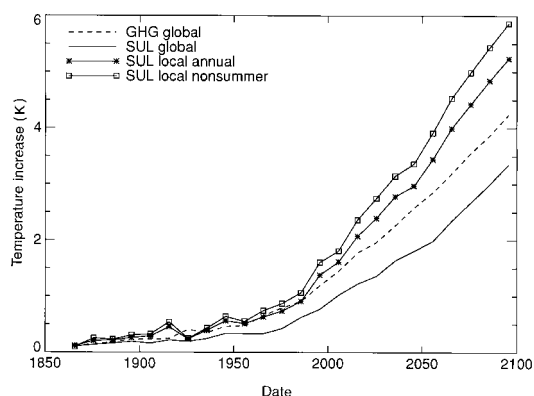


Figure 1 Simulated global-average temperature changes. From 1990 to 2100, carbon dioxide was increased in both GHG (dashed line) and SUL (solid lines) at 1% per year compounded, which is similar to the prescription of scenario IS92a of the Intergovernmental Panel on Climate Change (IPCC)¹⁵. SUL includes the additional effect of historical and future (IS92a) emissions of sulphate aerosols. All the temperatures shown are differences from the control integration, which has constant pre-industrial atmospheric conditions (nominally 1765). SUL and GHG began at 1860 with an instantaneous jump from the control. The simulated system adjusts to this with a characteristic timescale of about 6 years, so in a couple of decades it is very near to the state that would have resulted from a gradual increase of greenhouse gases before 1860. Starting in this way at 1860 leads to a loss of less than 10% in the time-integral of temperature 1860–1990. SUL and GHG provide a 'hindcast' of climate change since 1860, which Mitchell *et al.*³ compare with observations. They conclude that SUL gives a better match in both the global-average temperature change (about 0.5 K) and its geographical distribution in recent decades, whereas GHG overestimates the warming. However, both have discrepancies from the historical record. The local temperatures shown are averages over the glaciated regions only, where the annual average warming (asterisks) is larger than in the global average, and larger in non-summer months (squares) than in the annual average, as discussed in the text.

lower altitudes, where the temperature is above freezing for more of the year. Consequently they have a greater sensitivity to temperature change, and in some cases show substantial melting in non-summer months. The inclusion of the effects of seasonality and hypsometry on sensitivity is an important advantage of the model used here.

The glacier model excludes the effects of changes in precipitation, which could be important regionally (for example, the recent advance of glaciers in western Norway is related to increased precipitation), but temperature changes dominate on the large scale. Calculations with a mass-balance model⁸ indicate that a 20% decrease in precipitation would have the same effect as a temperature rise of 1 K. The temperature effect is likely to dominate; for instance, precipitation increases at only around 3% K⁻¹ in SUL and GHG north of 60° N.

The glacier model assumes the areas A_j are fixed, and hence that melt continues indefinitely at a constant rate for a given climate. In

fact, of course, the areas should decrease, as the glaciers contract and eventually disappear. This assumption is a weakness for which, in our opinion, there is currently no satisfactory solution. For the heavily glaciated regions and Greenland, from which most of the melt derives, it is probably acceptable for the next several decades. Further into the future our results represent an upper limit, giving an overestimate of perhaps 25% in the total melt by the end of the next century⁹. Uncertainties in the precipitation data and in the derivation of the sensitivities of the glacier model probably amount to 15% in the total.

To couple the models, time series of ΔT_S and ΔT_N are extracted for each x_j and used as input to the glacier model to obtain dV/dt . The rate of change of global average sea level dh/dt is computed using the total ocean surface area A_0 as

$$\frac{dh}{dt} = -\frac{1}{A_0} \frac{dV}{dt}$$

and the global average sea-level rise with respect to $t = 0$ is obtained by integrating dh/dt over time. Calculated by this method, the sea-level rise due to glacier melt over 1860–1990 is 19 mm from SUL and 33 mm from GHG, similar to the figure of 27 mm obtained by Zuo and Oerlemans⁵ using observed temperatures and the same glacier-melt model, and to Meier's¹⁰ estimate of 28 mm for 1900–1961.

The contribution to global average sea-level rise from glacier melt between 1990 and 2100 is 132 mm from SUL, 182 mm from GHG; the former is comparable with values of 120 mm and 160 mm obtained using simple climate models¹. The estimated present total volume of glaciers is equivalent to ~500 mm of sea-level rise¹, so by the end of the next century our predictions indicate that more than a quarter will have been lost. For comparison, sea-level rise from thermal expansion calculated by HADCM2 over the same period is 225 mm in SUL, 299 mm in GHG.

The largest contributions to total glacier melt derive from north-west America (43% of the total in SUL) and central Asia, whereas the intensively studied glaciers of the Alps contribute only about 1% of the total. All regions show less melting in SUL than in GHG, but the reduction is not uniform. Central Asia is significantly less important in SUL (23%) than in GHG (30%). This can be explained by the pattern of sulphate aerosol emissions, which in the scenario used is highly concentrated in the industrialized area of southeast Asia by the middle of the next century, reducing the temperature rise in this region relative to elsewhere.

Because the local seasonal temperature changes are approximately proportional to the global annual average $\Delta \bar{T}_A(t)$, there is a nearly linear relationship between dh/dt and $\Delta \bar{T}_A$. This gives 0.63 mm yr⁻¹ K⁻¹ for both SUL and GHG as our best estimate of the sensitivity to average temperature change of the glacier contribution to sea-level rise.

We repeat the calculation using the temperature change $\Delta T_A(x,t)$ averaged over the annual cycle at each location in place of both ΔT_S and ΔT_N . The result is 164 mm for SUL and 219 mm for GHG for 1990–2100, over 20% greater than from the first method. The reason for this has two parts. First, the annual average temperature rise in high northern latitudes, where most of the glaciers are, is greater than the summer temperature rise (Fig. 1), because there are additional feedbacks^{11,12} increasing the temperature rise in non-summer seasons. Second, most glaciers are more sensitive to summer than to non-summer warming, because a rise in temperature causes less increase in melt if the temperature remains low. These two facts together mean that the second calculation increases summer melt by more than it reduces non-summer melt. This effect is strongest for the Canadian and Siberian Arctic, less for Scandinavia and northwest America (Alaska, the Rockies and so on), whose comparatively maritime west-coast climates have a weaker seasonal contrast, and unimportant for the relatively low-latitude glaciers of central Asia (such as in the Himalayas).

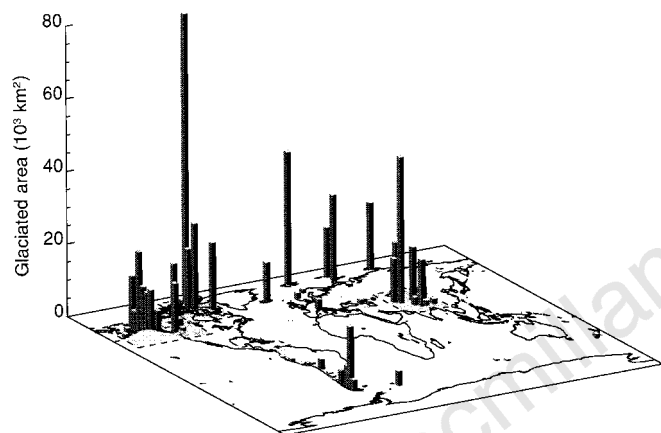


Figure 2 The locations of the 100 glaciated regions^{4,5}, excluding the ice sheets of Greenland and Antarctica. Each glaciated region is shown in its nearest AOGCM grid-box; some grid-boxes contain more than one. The three rectangular shaded areas are those we refer to as 'northwest America', the 'Canadian Arctic' and 'central Asia'. The precipitation characterizes the climate regime, which has a profound influence on the glacier mass-balance sensitivity. For instance, in the cold dry climate of the Canadian Arctic, the average magnitudes of summer and non-summer sensitivities are 0.15 and 0.01 mm yr⁻¹ K⁻¹ (expressed in terms of contribution to sea-level rise), whereas in the northwest American area, which is at lower latitude and affected by the nearby Pacific, there is much more non-summer melting, and the corresponding figures are 0.32 and 0.22. Iceland's mid-ocean location gives its ice caps a relatively mild and wet climate, with resulting sensitivities of 0.46 and 0.51.

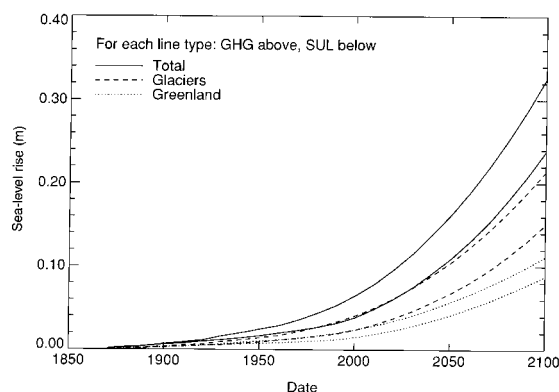


Figure 3 Contributions to global-average sea-level rise. Glaciers (dashed lines); Greenland (dotted); and their total (solid). Results are shown for both SUL and GHG; GHG gives the upper line in each case.

We perform the calculation a third time using ΔT_A at all locations and times of year. In this case, the result for 1990–2100 for SUL is 109 mm, GHG 149 mm, almost 20% less in each case than from the first method. This is because ΔT_A is less than the local temperature change for most glaciers, as the warming is generally larger over land than sea, and is greater in northern high latitudes.

Most of the water on land resides in the Greenland and Antarctic ice sheets, but the uncertainty about their state of mass balance is as large as the current observed rate of sea-level rise. However, it is relevant to consider the perturbations that might arise from anthropogenic climate change.

The Greenland ice sheet is similar to other high-latitude ice caps in that increased ablation will be the dominant effect of climate change on the mass balance. Therefore we extend the glacier model by defining four additional regions to cover Greenland, corresponding to different climate regimes¹³. They give a total sea-level rise of 76 mm for 1990–2100 in SUL, 93 mm in GHG. This is only about half the size of the glacier melt in each case (Fig. 3), despite the vastly greater area of the ice sheet, because its high latitude and altitude mean that its average surface temperature will remain low. Expressed as a temperature sensitivity, the contribution from Greenland to sea-level rise is $0.35 \text{ mm yr}^{-1} \text{ K}^{-1}$ in SUL and $0.30 \text{ mm yr}^{-1} \text{ K}^{-1}$ in GHG. Various other estimates¹ have been made of this sensitivity, mostly lying within a range of $0.30 \pm 0.15 \text{ mm yr}^{-1} \text{ K}^{-1}$, an uncertainty of 50%. As with mountain glaciers, we find that the total is increased by the use of ΔT_A , but reduced with ΔT_{ice} .

The Antarctic ice sheet experiences little ablation in either the current or future climates. Accumulation is mainly balanced by calving of icebergs, at a rate which is unlikely to change substantially over the next century, because it responds on the long timescale of ice-sheet dynamics. But precipitation over Antarctica apparently increases strongly with temperature, so climate change in Antarctica will make a negative contribution to sea level, as a consequence of the greater accumulation which will occur in a warmer climate. The sensitivity has been estimated¹ as $-0.30 \pm 0.15 \text{ mm yr}^{-1} \text{ K}^{-1}$, which would result in a sea-level fall of 79 mm over 1990–2100 with the temperature changes predicted by SUL, roughly cancelling the contribution from Greenland, as other studies have also suggested¹⁴. □

Received 7 April; accepted 18 November 1997.

1. Warrick, R. A., Le Provost, C., Meier, M. F., Oerlemans, J. & Woodworth, P. L. In *Climate Change 1995. The Science of Climate Change* (eds Houghton, J. T. et al.) 359–406 (Cambridge Univ. Press, 1996).
2. Johns, T. C. et al. The Second Hadley Centre coupled ocean–atmosphere GCM: Model description, spinup and validation. *Clim. Dyn.* **13**, 103–134 (1997).
3. Mitchell, J. F. B., Johns, T. C., Gregory, J. M. & Tett, S. F. B. Climate response to increasing levels of greenhouse gases and sulphate aerosols. *Nature* **376**, 501–504 (1995).
4. Oerlemans, J. in *Ice in the Climate System* (ed. Peltier, W. R.) (Springer, Berlin, 1993).
5. Zuo, Z. & Oerlemans, J. Contribution of glacier melt to sea level rise since AD 1865: a regionally differentiated calculation. *Clim. Dyn.* **13**, 835–845 (1997).
6. Kattenberg, A. et al. in *Climate Change 1995. The Science of Climate Change* (eds Houghton, J. T. et al.) 285–358 (Cambridge Univ. Press, 1996).
7. Oerlemans, J. & Fortuin, J. P. F. Sensitivity of glaciers and small ice caps to greenhouse warming. *Science* **258**, 115–117 (1992).
8. Oerlemans, J. A model for the surface balance of ice masses: Part I: Alpine glaciers. *Z. Gletscherkunde Glazialgeol.* **27/28**, 63–83 (1991).
9. Oerlemans, J. et al. Modelling the response of glaciers to climate warming. *Clim. Dyn.* (in the press).
10. Meier, M. F. Contribution of small glaciers to global sea level. *Science* **226**, 1418–1421 (1984).
11. Ingram, W. J., Wilson, C. A. & Mitchell, J. F. B. Modeling climate change: an assessment of sea ice and surface albedo feedbacks. *J. Geophys. Res.* **94**, 8609–8622 (1989).
12. Mitchell, J. F. B., Manabe, S., Meleshko, V. & Tokioka, T. in *Climate Change: The IPCC Scientific Assessment* (eds Houghton, J. T., Jenkins, G. J. & Ephraums, J. J.) 131–172 (Cambridge Univ. Press, 1990).
13. Oerlemans, J. The mass balance of the Greenland ice sheet: sensitivity to climate change as revealed by energy-balance modelling. *The Holocene* **1**, 40–49 (1991).
14. Thompson, S. L. & Pollard, D. Greenland and Antarctic mass balances for present and doubled atmospheric CO₂ from the GENESIS version-2 global climate model. *J. Clim.* **10**, 871–899 (1997).
15. Leggett, J., Pepper, W. J. & Swart, R. J. in *Climate Change 1992: The Supplementary Report of the IPCC Scientific Assessment* (eds Houghton, J. T., Callander, B. A. & Varney, S. K.) 69–96 (Cambridge Univ. Press, 1992).

Acknowledgements. R. L. H. Essery, W. J. Ingram and J. F. B. Mitchell made useful comments on the manuscript. J. A. Lowe helped with the calculation of thermal expansion. This work was partly supported by the UK Department of the Environment.

Correspondence should be addressed to J.G. (e-mail: jmgregory@meto.gov.uk).

Oceanic signals in observed motions of the Earth's pole of rotation

Rui M. Ponte*, Detlef Stammer† & John Marshall†

* Atmospheric and Environmental Research, Inc., 840 Memorial Drive, Cambridge, Massachusetts 02139, USA

† Department of Earth, Atmospheric, and Planetary Sciences, Massachusetts Institute of Technology, Cambridge, Massachusetts 02139, USA

Motion of the Earth's pole of rotation relative to its crust, commonly referred to as polar motion, can be excited by a variety of geophysical mechanisms¹. In particular, changes in atmospheric wind and mass fields have been linked to polar motion over a wide range of timescales, but substantial discrepancies remain between the atmospheric and geodetic observations^{1–4}. Here we present results from a nearly global ocean model which indicate that oceanic circulation and mass-field variability play important roles in the excitation of seasonal to fortnightly polar motion. The joint oceanic and atmospheric excitation provides a better agreement with the observed polar motion than atmospheric excitation alone. Geodetic measurements may therefore be used to provide a global consistency check on the quality of simulated large-scale oceanic fields.

Measurements collected through a variety of observational techniques have firmly established the existence of a wide spectrum of variability in the motion of the Earth's pole. Our planet as a whole conserves its angular momentum except for the known effects of external torques associated with lunisolar tides. Thus, the observed variability in polar motion, measured in the reference frame of the crust and mantle to which instruments are attached, results from angular-momentum exchanges between the mantle and the other main components of the Earth's dynamic system, including the atmosphere and the oceans. The changes in the angular momentum of the last two components may be associated with changes in either their mass fields, hence altering their moments of inertia, or their motion fields relative to the crust. Relevant for polar motion are the changes in the angular-momentum components about the two equatorial axes⁵—conventionally taken to point towards the Greenwich and 90° E meridians.

Taking advantage of the quality of available atmospheric operational analysis systems—which involve the combination of global atmospheric data sets and state-of-the-art numerical models to achieve an optimal estimation of the three-dimensional atmospheric state every 6 or 12 hours—a number of studies^{1–4} have established a clear relation between variable wind and mass fields and polar motion, for seasonal and shorter timescales. The correlation between atmospheric and geodetic time series, though significant, was however far from perfect, and most studies have suggested the potential importance of other sources of excitation, with the oceans being considered prime candidates.

Early attempts at determining the role of the ocean in the excitation of seasonal polar motion^{6,7}, based on models with simplified dynamics, very coarse resolution, no ocean-bottom relief, and limited geographical extent, were necessarily inconclusive because of the nature of the simplifying modelling assumptions. In the past decade, however, ocean modelling has progressed immensely, due to improvements in model formulation, external atmospheric forcing field, and computing power. Although an ocean operational analysis system equivalent to those available for the atmosphere has yet to be developed, several global ocean modelling efforts are currently underway. Recently, general circulation models based on full dynamics and thermodynamics have been reported to